2019 Conference
Earthquake risk and engineering towards a resilient world
9-10 September 2019, Greenwich, London

DEVELOPING FINITE ELEMENT MODELS FOR REINFORCED CONCRETE IMPACT ASSESSMENT IN UK ABWR NUCLEAR POWER PLANT

Will Shiliang LI[1], Andrew RUSHTON[2], Leonardo FELICIANI[3], Elliot PYE[4]&Takashi SUMIKAWA[5]

Abstract: *In the UK Advanced Boiling Water Reactor (ABWR) nuclear power plant design, reinforced concrete (RC) divisional barriers serve principal nuclear safety functions as they physically segregate the trains that deliver independent nuclear Fundamental Safety Functions (FSFs). They may be subjected to impact loading from internal hazards including dropped load, pipe whip, and missile impact. These impact loadings could potentially lead to serious safety consequences. Therefore, the RC divisional barriers must be substantiated against these hazard loadings. However, calculating the effect of impact loadings on RC structures is a challenging subject. It requires computing the complex non-linear dynamic behaviour of both the projectile and the RC target and can involve different damage modes such as concrete cracking, crushing, penetration, perforation, scabbing, bending and reaction shear. While a number of research projects have investigated this topic using both empirical and analytical methods, no clearly defined methodology specifying modelling parameters is currently available. This paper describes a study that reviewed well established research projects and design codes, standards, and guidance. A finite element modelling methodology using LS-DYNA was developed to predict the main structural response modes of RC structures under impact loading, including concrete crushing, bending deformation and reaction shear. The paper presents the validation of the finite element modelling methodology using a combination of experimental and empirical results.*

Introduction

The UK ABWR incorporates redundant and diverse Structures, Systems and Components (SSCs) to deliver its FSFs. Predominantly, these SSCs are physically segregated by barriers in the form of RC walls and slabs. The barriers, referred to as Class 1 Divisional Barriers, must be designed to withstand internal hazards and generally contain the effects within its originating safety division, hazard compartment or room; thereby protecting essential SSCs in adjacent safety divisions, compartments or rooms.

The behaviour of RC structures under impactive loading must consider both the local and global (or overall) structural response, as discussed in the R3 Impact Assessment Procedure. Both local and global response will occur in the same transient event, although one or the other may be dominant. While the R3 Impact Assessment Procedure gives comprehensive guidance to assess local effects (e.g. perforation and scabbing), no detailed methods for global assessment are provided.

Impact loadings on RC structures are challenging to analyse for several reasons, including:

- The complex non-linear dynamic behaviour of both the barrier and the projectile.
- The modelling of contact during the impact.
- The composite material models required to simulate the behaviour of reinforced concrete.

The approach for the UK ABWR was to assess local effects using empirical equations from the R3 Impact Assessment Procedure, and to use finite element analysis (FEA) to assess global

[1] Mr, SNC-Lavalin, Bristol, UK, Will.Li@atkinsglobal.com
[2] Mr, SNC-Lavalin, Bristol, UK
[3] Mr, SNC-Lavalin, Bristol, UK
[4] Mr, Hitachi-GE Nuclear Energy Ltd., Hitachi, Japan
[5] Dr, Hitachi-GE Nuclear Energy Ltd., Hitachi, Japan

effects. Previous studies showed that simplified methods were not suitable for the full range of impact scenarios. An FEA methodology was required to efficiently analyse and assess the global structural response for impact scenarios ranging from small, high velocity deformable projectiles to large, low velocity, non-deformable projectiles. The ductility demand and reaction shear needed to be assessed against acceptance criteria from established codes and standards such as ACI 349. The limitations of the FEA modelling methodology need to be understood.

LS-DYNA is a well-established FEA software package which has been used to analyse a large variety of impact scenarios in different industries (Murthy et al. 2010, Van Dorsselear et al. 2011, Terranova and Whittaker 2018). There are a number of user-developed material constitutive law formulations and parameters within the package that are appropriate for different applications. A wide range of research and industrial projects have adopted the software to assess impact loadings on RC structures. However, a clearly defined benchmark specifying modelling parameters and evaluating the model's accuracy is not currently available. To bridge this gap, this project developed an LS-DYNA FEA modelling methodology by adopting a specific group of modelling parameters, conducting model validation against a range of studies and calculating the discrepancies for each study.

A literature review was undertaken using well-established research publications, design codes and standards. The literature which was subsequently adopted for the FEA validation included IRIS 2012 Report, Delhomme et al. 2007, Gupta and Collins 2001, R3 and ACI 318-08. To investigate the model's accuracy, LS-DYNA was used to replicate the published scenarios. The discrepancy was calculated by comparing the FEA results to the observed experimental data, or in some cases with calculations based on design codes and standards.

The performance and accuracy of the finite element (FE) model were investigated for the following key aspects: bending capacity, bending deformation and reaction shear capacity. Studies considering local effects such as concrete penetration (crushing) and missile deformation were also conducted as these can significantly influence the global structural response.

The validation aspects and the corresponding validation case numbers are listed in Table 1. Additional cases were created with minor variations to investigate specific aspects, including reinforcement beam element definition, mesh density and missile impact velocity.

Aspect	**Case**
Reaction shear capacity	Case 1, Case 3
Global bending capacity	Case 2, Case 5, Case 7
Global bending deformation	Case 5, Case 7
Concrete penetration (crushing)	Case 4
Missile deformation	Case 5
Concrete perforation	Case 6

Table 1. Validation aspects and cases

Model Validation

Case 1 Concrete Beam Shear

Case 1 is a simply supported RC beam with a point load acting at the mid-span. The beam was designed to have a shear capacity lower than its bending capacity. With the partial material and load factors taken as 1.0, the ACI 318 shear capacity was calculated to be 504kN. Table 2 provides a summary of the beam information and the FEA shear capacity.

Beam dimension	**Bending reinforcement diameter**	**Bending reinforcement spacing**	**Shear reinforcement**	**Concrete cover to reinforcement**	**FEA shear capacity**
0.5 x 0.5 x 4m	26mm	100mm	None	50mm	504kN

Table 2. Case 1 FE model summary

In the FEA model, the concrete was modelled using the eight-node hexahedral solid elements with each side 50mm long. The steel reinforcement was modelled using 50mm long Hughes-Liu formulation beam elements.

Case 1a was created to investigate the effect of changing the reinforcement element definition to a truss element.

One of the aims of this project is to understand the feasibility of using a single concrete material model and its potential limitations. Studies such as Youcai et al. 2012 and Terranova and Whittaker 2018 have compared different concrete models available within LS-DYNA. It was concluded that the constitutive model for *MAT_CSCM_CONCRETE (MAT159) is a versatile concrete material model that would be straightforward to use in this study. This material model has been developed to predict the dynamic behaviour of concrete structures (FHWA-HRT-05-062, FHWA-HRT-05-063). This concrete model requires as a minimum the following parameters to model normal strength concrete: unconstrained compressive strength, mass, density and maximum aggregate size. The model can also account for the erosion of elements (i.e. an element loses all of its strength and stiffness) when certain criteria are met. This was implemented based on principal and shear strain values and was confirmed as being reasonable through comparison to previous projects, research publications including IRIS 2012 and sensitivity studies. The material model parameters for Case 1 are summarised in Table 3. Note that the maximum aggregate size was assumed to be 16mm for all the tests.

Property	**Concrete**	**Reinforcement**	**Unit**
Element definition	*SECTION_SOLID	*SECTION_BEAM	N/A
Material model	*MAT_CSCM_CONCRETE	*MAT_PLASTIC_KINEMATIC	N/A
Young's modulus	Not input	2.0×10^5	MPa
Tangent modulus	Not input	840	MPa
Poisson ratio	Not input	0.3	N/A
Tensile strength	Not input	500	MPa
Failure strain	Not input	0.05	N/A
Compressive strength	35	Not input	MPa
Density	2550	7850	kg/m^3
Concrete-reinforcement coupling	*CONSTRAINED_LAGRANGE_IN_SOLID		N/A

Table 3. Case 1 key FE model parameters

As shown in Figure 1, appropriate boundary conditions were used to simply support the beam at its ends and a prescribed displacement was applied to the beam at its midspan. The right hand side of Figure 1 shows the reinforcement modelled in Case 1, where only bending reinforcement was modelled (shown in red). The coupling of the concrete and reinforcement elements was achieved by using the card *CONSTRAINED_LAGRANGE_IN_SOLID. This type of coupling has been widely employed in a variety of projects (IRIS_2012 Report, Murthy et al. 2010, Rabeson et al. 2016). It allows the reinforcement and concrete elements to be constructed independently, and the mesh generation phase is more efficient than building a model with shared nodes.

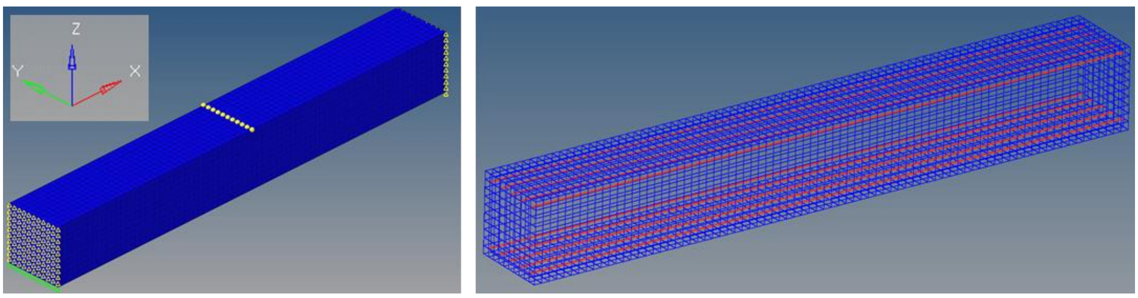

Figure 1. Case 1 FE model

As summarised in Table 10, the FEA shear capacity is the same as the ACI 318 calculation. For Case 1a, where truss element definition is used for reinforcement, the FEA shear capacity is 537kN, which is 6% higher than the ACI 318 calculation. It was found that Case 1a took approximately 40% less time to analyse, which indicates that using truss elements is less expensive in terms of computational time but is less accurate than using beam elements. Subsequent cases used beam elements to model the steel reinforcement.

Case 2 Concrete Beam Bending

Case 2 is similar to Case 1 and was used to validate the bending behaviour of a simply supported RC beam under a point loading at its midspan. Shear reinforcement was modelled, and the bending reinforcement diameter was increased from 26mm to 32mm. Subsequently, beam capacity was increased and was limited by its bending capacity of 821kN according to an ACI 318 calculation. Other material parameters were the same as specified in Table 3, including “beam” definition for the reinforcement elements.

The FEA bending capacity for Case 2 is 1042kN, which is about 20% higher than the ACI 318 calculation. This discrepancy was considered reasonable because the FEA steel reinforcement material model included a tangent modulus to represent strain hardening, whereas the ACI 318 calculation assumed perfectly plastic behaviour with zero tangent modulus.

Case 3 Concrete Column Shear

Case 3 was undertaken to compare the FEA shear capacity against physical experiments which were conducted by Gupta and Collins 2001. The physical experiments tested 24 RC columns with different concrete strengths loaded under various combinations of axial compression and shear. Case 3 considers the “PC7” test in Gupta and Collins 2001, where no axial load was applied to the column and a shear capacity of 387kN was measured.

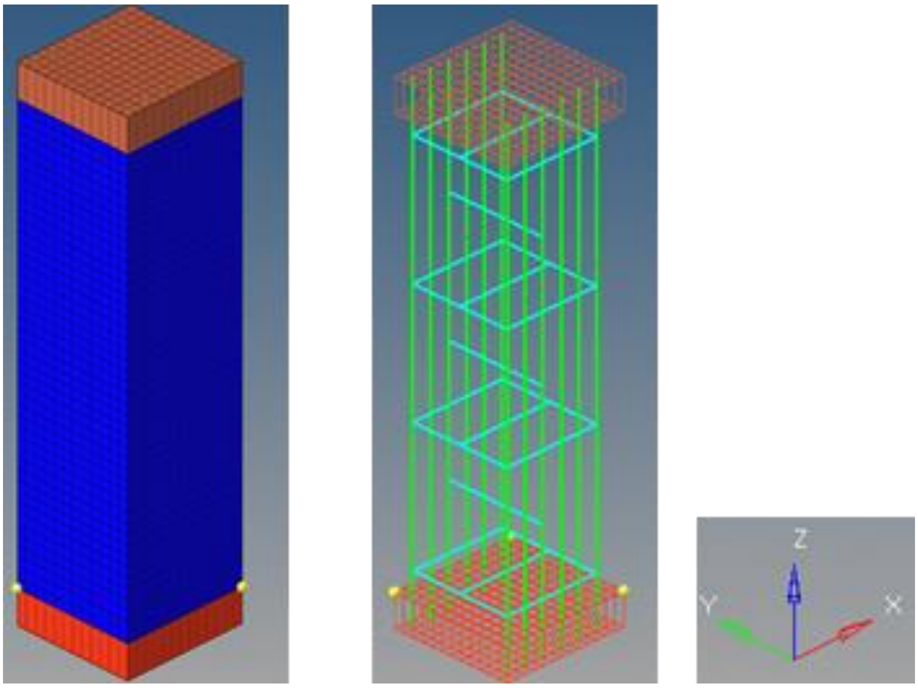

Figure 2. Case 3 FE model

Figure 2 presents the geometry model for Case 3. In the figure, two rigid bodies are attached to the top and bottom of the column. The bottom rigid body is fixed, and the top rigid body rotation is constrained. A horizontal displacement was applied to the top rigid body, putting the column in double bending, until the maximum shear capacity of the RC column was reached.

The same material models as Case 1 were used, although the reinforcement and concrete coupling method was changed. *CONSTRAINED_LAGRANGE_IN_SOLID was found to have certain limitations to accurately simulate the column response. This has also been reported by Schwer 2014. Therefore, the nodes in the reinforcement were made coincident with nodes in the concrete and rigid body elements. Table 4 summarises the Case 3 model parameters that are different from Table 3.

The maximum FEA shear force in the column at mid-height was 406kN. Comparing this with the 387kN reported in Gupta and Collins 2001, the discrepancy is considered to be acceptable and is summarised in Table 10.

Property	Concrete	Reinforcement	Unit
Element definition	*SECTION_SOLID	*SECTION_BEAM	N/A
Tangent modulus	Not input	800	MPa
Tensile strength	Not input	487, 509	MPa
Failure strain	Not input	0.223, 0.129	N/A
Compressive strength	39.9	Not input	MPa
Concrete reinforcement coupling	Shared nodes merged		N/A

Table 4. Case 3 key FE model parameter summary

This case showed that the agreement between the test and FEA results was good where there was zero compressive force in the RC column. However, further studies showed that the discrepancies between test and FEA results increased when combined shear and compression were considered. This limitation is consistent with the conclusions in Youcai et al. 2012.

Case 4 Concrete Penetration

A significant proportion of missile impact energy can be absorbed by concrete crushing as the missile penetrates into the barrier and this energy absorption mechanism should be modelled realistically. This requires concrete crushing to be accurately represented by the concrete model over a range of impact velocities. The concrete material model was validated against empirical equations from the R3 Impact Assessment Procedure.

The concrete penetration (crushing) depth was calculated using R3 equations for a rigid 47kg cylindrical missile impacting a concrete slab at different velocities. The dimensions, impact velocity and the calculated penetration depths of the rigid missile are shown in Table 5. No steel reinforcement was modelled.

Case	Slab Dimensions	Missile Velocity	Missile Dimensions	Concrete penetrations
Case 4	2m x 2m x 0.25m	35m/s	0.168m diameter x 0.640m long	3.6mm
Case 4a		55m/s		8.5mm
Case 4b		110m/s		31.3mm

Table 5. Case 44a and 4btest details

As shown in Figure 3, the Case 4, Case 4a and Case 4b FE models were constructed with the same geometry but with different missile impact velocities as shown in Table 5. Both the missile and the concrete slab were modelled using eight node hexahedral solid elements. There were ten equal size elements through the thickness of the slab. The missile was defined as a rigid body so that no impact energy was absorbed by missile deformation.

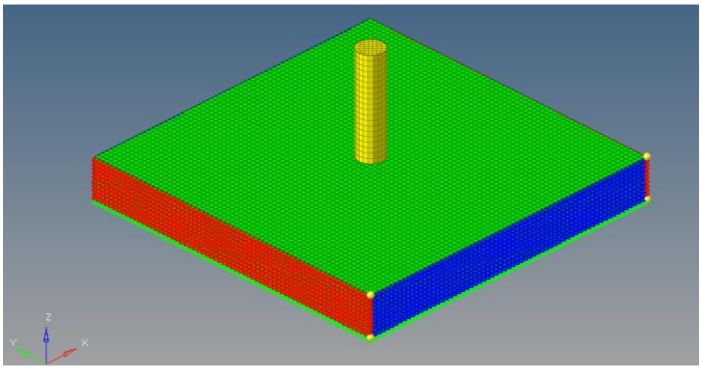

Figure 3. Case 4,4a and 4b FE model

The underside of the concrete slab was supported in the vertical direction. The slab was also restrained in the horizontal directions perpendicular to vertical faces to provide confinement condition for the concrete, as shown in red and blue in Figure 3. The same concrete model definitions as Case 1 were use. Details of the material input parameters are summarised in Table 6.

Property	Concrete	Missile	Unit
Element definition	*SECTION_SOLID	*SECTION_SOLID	N/A
Material model	*MAT_CSCM_CONCRETE	*MAT_RIGID	N/A
Young's modulus	Not input	2.0 x10^5	MPa
Poisson ratio	Not input	0.3	N/A
Compressive strength	35	Not input	MPa
Density	2300	3310	kg/m^3
Contact	*CONTACT_ERODING_SURFACE_TO_SURFACE		N/A

Table 6. Case 4, 4a and 4b FE model summary

The maximum penetrations from the FEA were calculated based on the displacement of the missile. The penetrations for Case 4, 4a and 4b were 3.3mm, 6.2mm and 14.5mm respectively. As summarised in Table 10, reasonable agreement was observed between the FEA and R3 predictions for Cases 4 and 4a. However, when the impact velocity was increased to 110m/s, the discrepancy was greater.

To investigate the effect of mesh density, Cases 4c and 4d were created by increasing the number of elements through the slab thickness from 10 to 20. These cases predicted penetration depths of 3.6mm and 25.5mm for impact velocities of 35m/s and 110m/s respectively, and showed that increasing the mesh density improved the accuracy. However, the run time was six times longer when the mesh density was doubled. Additional sensitivity studies were conducted for parameters including the "erode" value to ensure that the concrete material model definitions were appropriate.

Case 5 Slab Bending with a Deformable Missile

Case 5 replicated the IRIS 2010 B1 test to investigate the flexural behaviour of a target RC slab when impacted by a deformable (soft) missile. As presented in IRIS 2010, a thin-walled hollow stainless steel tube was used as the projectile impacting a 2m x 2m x 0.15m RC slab with shear reinforcement. The missile had a mass of 50kg and an impact velocity of 110m/s. A significant amount of axial buckling of the missile was observed in the experiment which dissipated a large amount of the impact energy, therefore the slab responded in a bending mode rather than undergoing localised punching shear.

In the FEA model, the concrete and reinforcement elements were modelled using the same material models as in Case 1. There were 10 equal sized solid elements through the thickness of the slab. The projectile was modelled using four node shell elements so that impact energy dissipation through missile buckling could be accurately simulated. Details of the parameters are shown in Table 7.

To realistically model the boundary condition of the test, the peripheral faces of the concrete slab were restrained in the Z direction. Additionally, the nodes along the bottom line of the peripheral faces along the X and Y directions were restrained in translational Y and X directions, respectively. This was to prevent potential unstable translational movement of the slab whilst avoiding unrealistic compressive strut effects in the slab.

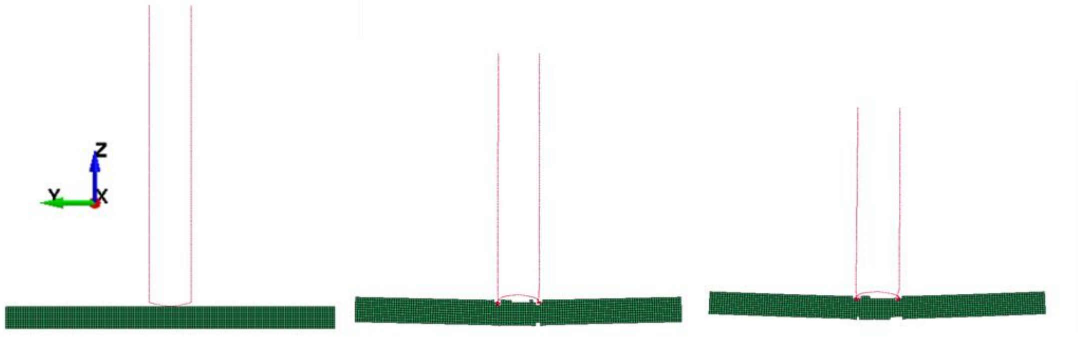

Figure 4. Case 5 during impact

Figure 4 shows images from beginning to the end of the Case 5 impact. The slab behaves in a relative ductile manner and there is limited localised damage at the impact location. This is consistent with the observed behaviour during the experiment. The maximum FEA displacement of the slab was 33mm, which was close to the experimental value of 29mm. In addition, the missile deformation was checked to see if the shell elements used in this analysis can accurately model the buckling behaviour during impact. The FEA results showed that the missile buckled by 39% of its length during the impact. Comparing with the experimental results where the missile deformed by 46%, the FEA results are considered sufficiently accurate.

Property	**Concrete**	**Reinforcement**	**Missile**	**Unit**
Element definition	*SECTION_SOLID	*SECTION_BEAM	*SECTION_SHELL	N/A
Material model	*MAT_CSCM_ CONCRETE	*MAT_PLASTIC_ KINEMATIC	*MAT_PLASTIC_ KINEMATIC	N/A
Young's modulus	Not input	2.0 x10^5	2.0 x10^5	MPa
Tangent modulus	Not input	840	840	MPa
Poisson ratio	Not input	0.3	0.3	N/A
Tensile strength	Not input	600	260	MPa
Failure strain	Not input	0.05	None	N/A
Strain rate	Not input	Cowper Symonds SRC=40.4 SRP=5	Cowper Symonds SRC=40.4 SRP=5	N/A
Compressive Strength	60	Not input	Not input	MPa
Density	2300	7850	14550	kg/m^3
Concrete-reinforcement coupling	*CONSTRAINED_LAGRANGE_IN_SOLID		N/A	N/A
Contact	*CONTACT_ERODING_SURFACE_TO_SURFACE			N/A

Table 7. Case 5 FE model summary

Case 6 Slab Perforation with a Rigid Missile

Case 6 replicated the IRIS 2010 P test which aimed to investigate the punching behaviour of a missile impact onto a RC slab. Comparing with Case 5, Case 6 uses a shorter but much stiffer missile with concrete infill. The missile had a mass of 47kg but a higher impact velocity of 135m/s, while the thickness of the slab was increased to 0.25m. The reinforcement in this test was 10mm diameter at 90mm spacing in both directions on both faces, and no shear reinforcement was provided. During the experiment, the slab was perforated with a large amount of scabbing occurring at the back face of the slab. The residual missile velocity was reported to be from 33.8m/s to 45.3m/s for repeated tests. Unlike the IRIS B1 test, no significant missile deformation was observed during the IRIS P test.

Property	**Concrete**	**Reinforcement**	**Missile**	**Unit**
Element definition	*SECTION_SOLID	*SECTION_BEAM	*SECTION_SOLID	N/A
Material model	*MAT_CSCM_ CONCRETE	*MAT_PLASTIC_ KINEMATIC	*MAT_PLASTIC_ KINEMATIC	N/A
Tensile strength	Not input	600	260	MPa
Density	2300	7850	14550	kg/m^3

Table 8. Case 6 FE model summary

Most of the FE model parameters in Case 6 were the same as Case 5. However, Case 6 modelled the missile using eight node hexahedral solid elements rather than using shell elements. This was designed to represent the "hard impact" condition. The modelling parameters different from Table 7 are presented in Table 8.

Results from the Case 6 FEA are shown in Figure 5 from the beginning to the end of the impact. In contrast to the missile behaviour in Case 5, where large missile deformations were observed, the solid missile in Case 6 undergoes a limited amount of deformation. The perforation damage in the FEA is consistent with the experimental observations.

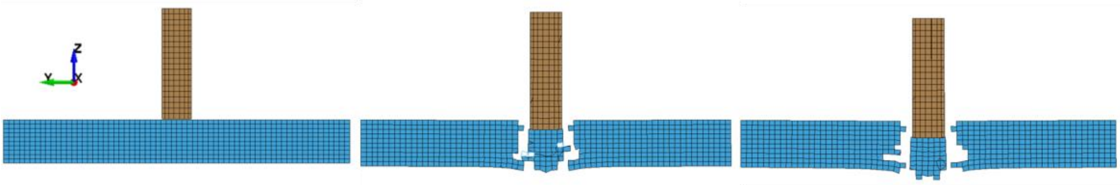

Figure 5. Case 6 during impact

The FEA residual missile velocity in Case 6 was 39m/s, which was within the range of experimental results. This suggested that the amount of internal energy dissipated in the slab during the perforation was accurately modelled by the FEA.

Case 7 Slab Bending with a Rigid Missile

Cases 7 and 7a constructed an FE model to replicate the Delhomme et al. 2007 experiments, where a 450kg concrete block was dropped onto a 12m x 4.8m x 0.28m RC slab from 15m and 30m, and the displacement of the slab was measured.

The left-hand side of Figure 6 shows the geometric model for the Delhomme test (Case 7). Both the projectile and the RC concrete slab were modelled using eight-node solid elements. There were ten equal size solid elements through the thickness of the slab. The longitudinal concrete edge faces were restrained in the transverse directions. The same concrete and reinforcement models as in Case 1 were used. Table 9 summaries the Case 7 model parameters that are different from Case 6.

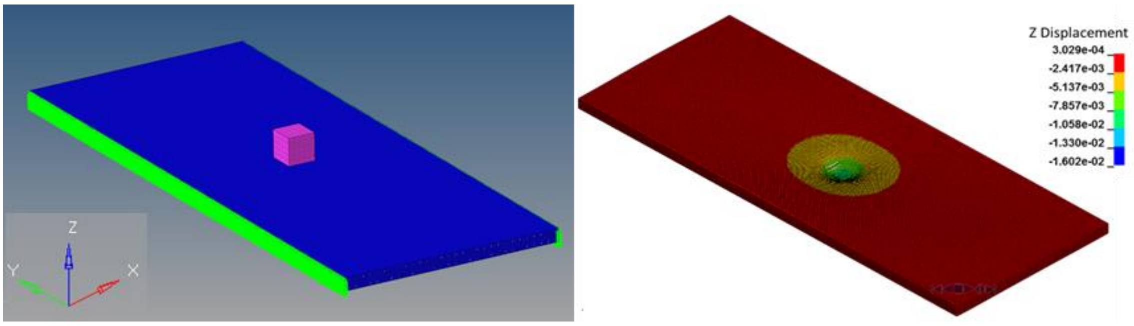

Figure 6. Case 6 model and its response during impact

Property	**Concrete**	**Reinforcement**	**Missile**	**Unit**
Material model	*MAT_CSCM_ CONCRETE	*MAT_PLASTIC_ KINEMATIC	*MAT_CSCM_ CONCRETE	N/A
Young's modulus	Not input	2.0 x10^5	Not input	MPa
Tangent modulus	Not input	840	Not input	MPa
Poisson ratio	Not input	0.3	Not input	N/A
Tensile strength	Not input	500	Not input	MPa
Failure strain	Not input	None	None	N/A
Strain rate	Not input	Cowper Symonds SRC=40.4 SRP=5	Not input	N/A
Compressive strength	30	Not input	30	MPa
Density	2300	7850	2300	kg/m^3

Table 9. Case 7 FE model parameter summary

The right-hand side of Figure 6 shows the deflection contour plot in the Z direction of the slab at the end of the impact for Case 7. It shows that most of the displacement of the slab was concentrated near the impact area, and no perforation occurred. This is consistent with the observations from the test. The maximum FEA displacement of the slab was 12mm, which was close to the experimental result of 14.5mm. Case 7a showed a similar response to Case 7. The maximum FEA displacement was 18mm, which was close to the experimental result of 23.2mm.

Conclusions

In this study, a FEA modelling methodology using LS-DYNA was developed to efficiently predict the main structural response modes of RC structures under impact loading, including concrete crushing, bending deformation and reaction shear. The discrepancies calculated in the validation studies are summarised in Table 10.

Case No.	Validation Aspect	Key Parameter	Discrepancy Measurement	Value
1	Shear capacity	Beam elements	$\frac{\text{FEA shear capacity} - \text{ACI shear capacity}}{\text{FEA shear capacity}}$	0%
1a		Truss elements		6%
2	Bending capacity	-	$\frac{\text{FEA bending capacity} - \text{ACI bending capacity}}{\text{FEA bending capacity}}$	5%
3	Shear capacity	Shear test	$\frac{\text{FEA shear capacity} - \text{Test shear capacity}}{\text{FEA shear capacity}}$	19%
4c	Concrete penetration (crushing)	35m/s impact	$\frac{\text{R3 penetration} - \text{FEA penetration}}{\text{R3 penetration}}$	0%
4a		55m/s impact		27%
4d		110m/s impact		8%
5	Slab bending	-	$\frac{\text{FEA slab displacement} - \text{Test slab displacement}}{\text{FEA slab displacement}}$	12%
5	Missile deformation	-	$\frac{\text{FEA missile deformation} - \text{Test missile deformation}}{\text{FEA missile deformation}}$	-21%
6	Slab perforation	-	$\frac{\text{FEA perforation energy} - \text{Test perforation energy}}{\text{FEA perforation energy}}$	0%
7	Slab bending	15m drop	$\frac{\text{FEA slab deformation} - \text{Test slab deformation}}{\text{Test slab deformation}}$	-19%
7a		30m drop		-22%

Table 10. Model validation summary

The following observations were made:

- Cases 2, 5 and 7 show that the FEA over-predicts the bending capacity and under-predict the bending deformation by up to 30%. This suggests that the FEA methodology may underestimate the ductility demand.
- Case 3 shows that the FEA over-predicts the shear capacity of reinforced concrete sections. However, this can be mitigated by assessing the FEA reaction shear estimates against design code shear capacities.
- Case 4 shows that the FEA under-predicts the concrete crushing depth compared to the R3 empirical equations. This means that the concrete crushing force will be overestimated. This will provide a conservative assessment of global effects as the reaction shear will also be overestimated and the impact energy will be absorbed by the global response in preference to the local (concrete crushing) response.
- Case 6 shows that the accuracy for concrete perforation was reasonable.

The FEA limitations and the discrepancies between the test results and the FEA analyses and limitations were taken into account when assessing UK ABWR impact hazards.

Care should be taken when modelling the interaction between the concrete and steel reinforcement elements, particularly where there are high bond forces close to the boundaries of the model.

In summary, the material model *MAT_CSCM_CONCRETE can simulate concrete behaviour with reasonable accuracy under impact loading conditions where the concrete confinement is relatively low. At least ten elements are required through the thickness of the concrete barrier to model the structural behaviour with sufficient accuracy. However, when assessing impact scenarios that are dissimilar to the cases considered in this study, additional element size/mesh density sensitivity studies should be undertaken.

References

ACI 318-08:*Building Code Requirements for Structural Concrete*, American Concrete Institute, ISBN 9780870312649, 2007

ACI 349-13:*Code Requirements for Nuclear Safety-Related Concrete Structures (ACI 349-13) and Commentary*, American Concrete Institute, ISBN 9780870318948, 2014

Delhomme F, Mommessin M, Mougin J P, Perrotin P, Simulation of a Block Impacting a Reinforced Concrete Slab with a Finite Element Model and a Mass-spring System, Engineering Structures 29 (2007) 2844-2852, March 2007

FHWA-HRT-05-062: User Manual for LS-SYNA Concrete Material Model FHWA-HRT-05-062, US Department of Transportation, Federal Highway Administration, Research, Development and Technology Turner-Fairbank Highway Research Centre, May 2007

FHWA-HRT-05-063: Evaluation of LS-SYNA Concrete Material Model 159, US Department of Transportation, Federal Highway Administration, Research, Development and Technology Turner-Fairbank Highway Research Centre, May 2007

Gupta P Rand Collins M P, Evaluation of Shear Design Procedures for Reinforced Concrete Members under Axial Compression, ACI Structural Journal Technical Paper 98-S51, July 2001

IRIS_2012Improving Robustness Assessment Methodologies for Structures Impacted by Missiles Final Report, OECD Nuclear Energy Agency (NEA) Committee on the Safety of Nuclear Installations, August 2014

Issac Rabeson, Thierry Marmeth, Fatimata Traore, Bruno Moins, SilvanoErlicher, Reinforced Concrete Slab Perforation: Experimental vs. Numerical Behaviour, 3rd Conference on Technological Innovations in Nuclear Civil Engineering, September 2016

Len Schwer, Modeling Rebar: The Forgotten Sister in Reinforced Concrete Modeling, 13th International LS-DYNA Conference, Constitutive Modeling, 2014

LS-DYNA Theory Manual, Livermore Software Technology Corporation (LSTC), ISBN 0-9778540-0-0, March 2006

MurthyA R, Palani G S and IyerN R, Impact Analysis of Concrete Structural Components, Defence Science Journal, May 2010

R3:Impact Assessment Procedure, Magnox North Ltd. & British Energy Generation Ltd, 2009

TerranovaB, WhittakerA, Benchmarking Concrete Material Models Using the SPH formulation in LS-DYNA, June 2018

Van DorsselearN, LapoujadeV, NahaG, Tarllao F, RambachJM, Impact Simulations on Concrete Slabs: LS-OPT Fitting Approach, 8th European LS-DYNA Users Conference, May 2011

Wu Y, CrawfordJ E, MagallanesJ M, Performance of LS-DYNA Concrete Constitutive Models, 12th International LS-DYNA Users Conference, 2012